NIH Public Access
Author Manuscript
Neuroimage. Author manuscript; available in PMC 2014 January 15.

Published in final edited form as:
Neuroimage. 2013 January 15; 65: 288–298. doi:10.1016/j.neuroimage.2012.09.075.

Influence of the fragile X mental retardation (*FMR1*) gene on the brain and working memory in men with normal *FMR1* alleles

Jun Yi Wang[1,3], **David Hessl**[2,3], **Christine Iwahashi**[5], **Katherine Cheung**[5], **Andrea Schneider**[2,4], **Randi J. Hagerman**[2,4], **Paul J. Hagerman**[2,5], and **Susan M. Rivera**[1,2,6]

[1]Center for Mind and Brain, University of California-Davis, Davis, CA

[2]Medical Investigation of Neurodevelopmental Disorders (MIND) Institute, University of California-Davis Medical Center, Sacramento, CA

[3]Department of Psychiatry and Behavioral Sciences, University of California-Davis, School of Medicine, Sacramento, CA

[4]Department of Pediatrics, University of California-Davis, School of Medicine, Sacramento, CA

[5]Department of Biochemistry and Molecular Medicine, University of California-Davis, School of Medicine, Sacramento, CA

[6]Department of Psychology, University of California-Davis, Davis, CA

Abstract

The fragile X mental retardation 1 (*FMR1*) gene plays an important role in the development and maintenance of neuronal circuits that are essential for cognitive functioning. We explored the functional linkage(s) among lymphocytic *FMR1* gene expression, brain structure, and working memory in healthy adult males. We acquired T1-weighted and diffusion tensor imaging from 34 males (18–80 years, mean ± SD = 43.6 ± 18.4 years) with normal *FMR1* alleles and performed genetic and working memory assessments. Brain measurements were obtained from fiber tracts important for working memory (i.e. the arcuate fasciculus, anterior cingulum bundle, inferior longitudinal fasciculus, and the genu and anterior body of the corpus callosum), individual voxels, and whole brain. Both *FMR1* mRNA and protein (FMRP) levels exhibited significant associations with brain measurements, with FMRP correlating positively with gray matter volume and white matter structural organization, and *FMR1* mRNA negatively with white matter structural organization. The correlation was widespread, impacting rostral white matter and 2 working-memory fiber tracts for FMRP, and all cerebral white matter areas except fornix and cerebellar peduncles and all 4 fiber tracts for *FMR1* mRNA. In addition, the levels of *FMR1* mRNA as well as the fiber tracts demonstrated significant correlation with working memory performance. While *FMR1* mRNA exhibited negative correlation with working memory, fiber tract structural organization showed positive correlation. These findings suggest that the *FMR1* gene is a genetic factor in common for both working memory and the brain structure, and has implications for our understanding of the transmission of intelligence and brain structure.

© 2012 Elsevier Inc. All rights reserved.

Correspondence: Susan Rivera, *Address:* Center for Mind and Brain, 267 Cousteau Place, Davis, CA 95618, *Phone*: 530.747.3802, *Fax*: 530.297.4603, srivera@ucdavis.edu.

Publisher's Disclaimer: This is a PDF file of an unedited manuscript that has been accepted for publication. As a service to our customers we are providing this early version of the manuscript. The manuscript will undergo copyediting, typesetting, and review of the resulting proof before it is published in its final citable form. Please note that during the production process errors may be discovered which could affect the content, and all legal disclaimers that apply to the journal pertain.

$watermark-text

$watermark-text

$watermark-text

$watermark-text

$watermark-text

$watermark-text

Keywords

FMR1; Diffusion tensor imaging; Working memory; Cognition; White matter; Tractography

Introduction

The fragile X mental retardation 1 (*FMR1*) gene encodes for the fragile X mental retardation protein (FMRP), a RNA-binding protein that regulates protein synthesis for activity-dependent synaptic development and plasticity (Bassell and Warren, 2008). Both *FMR1* mRNA and FMRP have been localized in the cell body, axons, and dendrites (Bassell and Warren, 2008; Devys et al., 1993). A newly published study (Darnell et al., 2011) reported that FMRP regulates the translation of approximately one-third of the proteins in the pre- and post-synaptic proteome, underscoring the critical role of *FMR1* in the development and maintenance of neuronal circuits.

In accordance with the importance of *FMR1* expression in brain development and function, abnormal levels of *FMR1* protein and mRNA have been found to lead to two independent brain disorders: fragile X syndrome and fragile X-associated tremor/ataxia syndrome (FXTAS) (Oostra and Willemsen, 2009). The dynamics of *FMR1* gene expression originate from expansion of the polymorphic CGG repeat in the 5' untranslated region of the gene, which normally ranges from 5–44 triplets (Verkerk et al., 1991). When CGG repeats expand beyond 200 triplets (termed the full mutation range), the promoter and CGG-repeat regions of the gene generally become hypermethylated, with consequent transcriptional and translational silencing (Pieretti et al., 1991); loss of FMRP expression results in fragile X syndrome (Devys et al., 1993), the most frequent single-gene caused intellectual disability (Crawford et al., 1999). Premutation alleles with CGG lengths between 55–200 triplets (Pieretti et al., 1991) produce slightly reduced protein, but significantly elevated *FMR1* mRNA (Tassone et al., 2000). Transcriptional upregulation of the expanded CGG-repeat alleles is known to be toxic to both neuronal and non-neuronal cells (Garcia-Arocena and Hagerman, 2010), and has also been demonstrated to cause altered neuronal connectivity in cultured neonatal mouse neurons, and altered neuronal differentiation and migration in embryonic mice (Chen et al., 2010; Cunningham et al., 2011). Elevated levels of the expanded CGG-repeat *FMR1* mRNA could thus have an impact on child development (i.e., could be the pathogenic basis for the neurodevelopmental phenotypes among carriers of premutation alleles) (Chonchaiya et al., 2011; Farzin et al., 2006), as well as the clear RNA toxicity associated with aging (Hagerman and Hagerman, 2004). Boys with *FMR1* premutation alleles are reported to have a higher risk of developing autism spectrum disorders and attention-deficit/hyperactivity disorders (Chonchaiya et al., 2011; Farzin et al., 2006), whereas older (adult) carriers of premutation alleles may develop FXTAS, typically after 50 years of age (Hagerman and Hagerman, 2004). Among the range of noted cognitive impairments, working memory has emerged as a consistent impairment associated with both the fragile X full mutation (Lanfranchi et al., 2009) and the premutation (Cornish et al., 2009; Hashimoto et al., 2011a).

Working memory is defined as a system that temporarily holds and manipulates a limited amount of information for the accomplishment of complex cognitive tasks such as comprehension, learning, and reasoning (Baddeley, 2000). Extensive research has been conducted to understand and localize this complex cognitive function. Working memory has been recognized as a central component of human intelligence (Wechsler, 1997a). It is highly heritable (Karlsgodt et al., 2010) and is affected in a number of neurogenetic disorders in addition to fragile X syndrome, including schizophrenia, 22q deletion syndrome, and autism spectrum disorders (Greene et al., 2008; Karlsgodt et al., 2011).

$watermark-text

$watermark-text

$watermark-text

Functional neuroimaging studies have identified a distributed neural network that mediates the function of working memory (Rama, 2008; Zimmer, 2008). This network encompasses both modality-specific cortical areas in the temporal, parietal, and occipital lobes for encoding sensory-motor information and supramodal regions in the frontal and parietal lobes for maintaining and manipulating task information. Structural MRI studies (Burzynska et al., 2011; Charlton et al., 2010; Sepulcre et al., 2009; Takeuchi et al., 2010; Vestergaard et al., 2011; Zahr et al., 2009) have also been conducted to search for white matter tracts serving as the structural backbone of the working memory network and reported the following fiber tracts as being associated with working memory performance: the superior longitudinal fasciculus (SLF; carrying the frontoparietal pathways), inferior longitudinal fasciculus (ILF; contains the superior parietal lobule pathway in Charlton et al., 2010), corpus callosum, fornix, cingulum, thalamic radiation, and cerebellar white matter.

Only one study (Hashimoto et al., 2011a) has investigated brain-mediated *FMR1* effect on working memory. This functional MRI study reported reduced activation during a verbal working memory task in core working memory areas--right ventral inferior frontal cortex and left premotor/dorsal inferior frontal cortex for both premutation carriers with and without FXTAS compared to healthy controls. In addition, the study detected a negative effect of CGG repeat length on the activation of right ventral inferior frontal cortex when the carriers with and without FXTAS were combined. Currently, the influence of *FMR1* expression on the brain and working memory in individuals with normal alleles remains unknown.

Accordingly, the principal-objective of the current study is to assess the functional linkage(s) among *FMR1* gene expression, the brain white and gray matter structure, and working memory performance in healthy adult males. To this end, we have acquired diffusion tensor imaging (DTI) (Basser and Pierpaoli, 1996; Mori et al., 1999) as well as T1-weighted MRI to perform an *in vivo* examination of macro- and micro-structures of the gray and white matter. We found that FMRP showed a significant positive correlation with gray matter volume, and *FMR1* mRNA showed a negative correlation with brain-level white matter structural organization. Both FMRP and *FMR1* mRNA exhibited correlations with DTI tractography- and voxel-based measurements, where higher FMRP and lower *FMR1* mRNA were associated with improved white matter structural organization. In addition, *FMR1* protein and mRNA levels as well as tractography measurements correlated significantly with working memory, demonstrating the close relationships between the *FMR1* gene, the brain structure, and working memory observable in normal populations.

Materials and Methods

Research participants

We recruited 37 healthy males from the local community, among which 26 were non-Hispanic Caucasian, 3 Hispanic Caucasian, 4 Asian, 3 with more than one race, and 1 of unknown ethnic background. None of the participants had neuropsychological disorders, prolonged loss of consciousness, brain infection, major psychiatric illness such as bipolar or schizophrenia, major chronic illness (cancer, liver disease, etc.), head trauma, a history of substance or alcohol abuse, or extensive T2-hyperintensive lesions or retinal damage due to diabetes or hypertension. While none of the younger males (< age 50) had diabetes or hypertension, 1 of the 13 older males (> 45 years) were diagnosed as having type II diabetes and 4 had hypertension. Structured Clinical Interviews for DSM-IV (SCID-I) revealed that at the time of the study, 4 participants had a mood and/or anxiety disorder and 14 had a past mood and/or anxiety disorder (lifetime). All participants signed informed consent and agreed to participate in the study. Local institutional review board at University of California, Davis approved the research protocol.

$watermark-text

$watermark-text

$watermark-text

Working memory assessments

Working memory performance was measured using the Working Memory subtests from Wechsler Memory Scales, Third Edition (WMS) (Wechsler, 1997b), which provides standardized, age-scaled scores. The average index score is 100, with standard deviation 15.

Molecular genetic measures

Genomic DNA was isolated from peripheral blood lymphocytes using standard methods (Qiagen, Valencia, CA). CGG repeat size was determined using real time polymerase chain reaction and Southern Blot analysis performed on an Alpha Innotech FluorChem 8800 Image Detection System (San Leandro, CA) as previously described (Filipovic-Sadic et al., 2010). *FMR1* mRNA was quantified on a 7900 Sequence detector (PE Biosystems) using the published method (Filipovic-Sadic et al., 2010; Tassone et al., 2000). FMRP level was measured utilizing a recently described sandwich Enzyme Linked ImmunoSorbent Assay for FMRP (Iwahashi et al., 2009), which quantifies the FMRP level directly rather than counting the proportion of cells with detectable staining in the commonly used immunocytochemistry method.

Neuroimaging data acquisition

We acquired DTI from 32/37 participants, the only imaging modality that allows us to examine white matter spatial organization *in vivo* (Basser and Pierpaoli, 1996; Mori et al., 1999). DTI measures spatial distribution of water diffusion in the brain which is constrained by brain tissues. In the white matter where axons form large fiber bundles and run in parallel, water molecules tend to diffuse more along than against fiber tracts. Based on this characteristic, the dominant diffusion direction is found by modeling the spatial distribution of water diffusion using tensors. From tensors, diffusion measurements are calculated including fractional anisotropy (FA) for measuring water-diffusion directionality and mean diffusivity (MD) for the amount of restriction to water diffusion due to the presence of brain tissues. Additional useful measurements include axial diffusivity (AD), the amount of diffusion along the dominant diffusion direction, and radial diffusivity (RD), the average diffusion perpendicular to the dominant diffusion direction. Although controversial, AD and RD have been proposed for differentiating compromised axon from myelin loss, with AD reduction indicating the former and RD elevation the latter (Song et al., 2002). After tensor calculation, fiber tracking is performed by connecting voxels with similar dominant diffusion direction to form DTI streamlines that can infer anatomical connections between brain regions.

Neuroimaging was performed on a Siemens Trio 3T MRI scanner with an 8-channel had coil (Siemens Medical Solutions, Erlangen, Germany). DTI data were acquired using an EPI sequence in 72 axial slices of 1.9 mm thickness without gap. The FOV was 243 mm, matrix 128×128, TR 11,900 ms, TE 92 ms, and flip angle 90°. The diffusion weighted images were obtained at *b*-value 700 s/mm^2 in 30 directions along with five images with minimum diffusion weighting. High-resolution T1-weighted 3D magnetization prepared rapid gradient echo (MPRAGE) images were also obtained from all 37 participants. The participants came from two separate studies and thus were scanned with two slightly different sequences. The younger participants (< 45 years, $N = 24$) were scanned in 192 sagittal slices of 1 mm thickness (no gap) with FOV 256 mm, 256 × 256 matrix, TR of 2,170 ms, TE of 4.82 ms, and 7° flip angle. The older participants (> 45 years, $N = 13$) were scanned in 208 sagittal slices of 0.95 mm thickness (no gap) with FOV 243 mm, 256 × 256 matrix interpolated to 512 × 512, TR of 2,500 ms, TE of 4.33 ms, and 7° flip angle.

$watermark-text

$watermark-text

$watermark-text

Image processing

Following image acquisition, we corrected eddy current and motion in DTI images and performed skull stripping (Smith, 2002) using software package FSL (www.fmrib.ox.ac.uk/fsl/, University of Oxford, UK). The subsequent tensor calculation, DTI map generation, and fiber tracking were conducted in DTI Studio (cmrm.med.jhmi.edu/, Johns Hopkins Medical Institute, Baltimore, MD). To ensure the successful reconstruction of small curvature tracts such as the uncinate fasciculus, the FA threshold was set to 0.18 and angle threshold 70°. A multiple regions-of-interest (ROI) approach was adopted to extract a tract of interest (Wakana et al., 2007; Wakana et al., 2004).

Four fiber tracts important for working memory were reconstructed and comprised the arcuate fasciculus, anterior cingulum, inferior longitudinal fasciculus (ILF), and the genu (CCg) and anterior body (CCab) of the corpus callosum. The fiber tracking methods have been described previously and have been tested for both inter-rater reliability and test-retest reliability (Wang et al., 2012a; Wang et al., 2011; Wang et al., 2012b). For the arcuate fasciculus, its three components were reconstructed according to Catani's definition (Catani et al., 2005), comprising the direct connection between the Broca's area with Wernicke's area, the anterior component linking the Broca's area with Geschwind's area, and the posterior component linking the Geschwind's area with Wernicke's area. Subsequently, the three components were combined to form arcuate fasciculus complex. A comparison of the anterior arcuate fasciculus with the superior longitudinal fasciculus (SLF) reconstructed following a published method (Thiebaut de Schotten et al., 2012) showed substantial overlapping between the anterior arcuate fasciculus and the third branch of SLF (SLFIII, Appendix Fig. 1). For the corpus callosum, only the genu (CCg) and anterior body (CCab) that have been shown to be important for working memory (Takeuchi et al., 2010; Zahr et al., 2009) were included in the analyses. Fiber regions were quantified using FA, MD, and tract volume (i.e. the number of voxels occupied by the streamlines of a fiber tract).

Volumes of the gray and white matter were estimated from the MPRAGE using the SIENAX function (Smith et al., 2002) from FSL. SIENAX is an automated tool that performs volume estimations for the gray matter, white matter, and CSF following the steps of brain extraction, affine-registration to MNI 152 space, tissue segmentation, and volume calculation. Another set of global brain values, the average FA and MD values of the white matter and the average MD of the gray matter, were obtained by superimposing gray and white matter masks on FA and MD maps generated from DTI Studio in subjects' native space. Firstly, the mean *b*0 images were calculated from DTI Studio and served as the input files for tissue segmentation. The mean *b*0 images were utilized in replacement of T1 scans to avoid imperfect co-registration between T1 and DTI images that commonly occurs in DTI images containing EPI-related image distortion. Secondly, tissue segmentation was performed using the Segment module from Statistical Parametric Mapping Software (SPM5) (Wellcome Department of Imaging Neuroscience, London, UK) running on MATLAB version 7.10.0 (The Mathworks, Inc., Natick, MA, USA). The Segment module integrates tissue classification, bias correction, and nonlinear warping to generate tissue probability maps of the gray and white matter and CSF from which binary masks of the gray and white matter were generated by setting the threshold at 94% probability using an in-house MATLAB script. The white matter volumes calculated from the SPM5 masks showed excellent associations with the white matter volumes, estimated using FSL Sienax, while the association between the gray matter volumes was not significant (Appendix Fig. 2). Thirdly, the same MATLAB script was utilized to mask the FA and MD maps with the gray and white matter masks to calculate the averaged DTI values for the gray and white matter.

Voxel-based analysis was conducted using Tract-Based Spatial Statistics (TBSS) from FSL. TBSS generates a skeleton from the core of the white matter that is least affected by

imperfect image registration and partial volume effect, the two common issues during the process of group analysis. Firstly, FA, MD, AD, and RD maps were generated from DTI images using the FDT toolbox from FSL. Secondly, all FA images were nonlinearly registered to FMRIB58_FA standard-space image and then affine transformed to MNI152 space. The resulting transformation matrix was also applied to other DTI images. Thirdly, the mean FA map was generated and thinned to create the mean FA skeleton. Then FA threshold 0.2 was applied to create a skeleton mask. Finally, the aligned DTI maps were projected onto the skeleton mask to generate the images for individual participants to be used in the statistical analysis.

Statistical analysis

For the DTI data, the global measurements were estimated as the average FA or MD over the gray or white matter. The FA and MD for individual fiber tracts were calculated in DTI Studio as the average FA and MD values for all voxels occupied by the reconstructed DTI-streamlines, with the voxels occupied by multiple streamlines counted multiple times. To assess the correlation between the genetic and DTI data, multiple linear regression was employed to predict individual tractography measurements from either *FMR1* mRNA or FMRP. Age was used as a covariate to account for the high correlation between age and tractography measurements. The significant association was verified in TBSS using the randomize tool with threshold-free cluster enhancement. The same regression model was also used to predict global DTI and volume measurements from the genetic data.

The association between imaging data and working memory performance was assessed in multiple linear regression using individual tractography measurements as the independent variable and age as a covariate to predict working memory scores. In addition, to predict working memory scores from the overall connectivity strength of the working memory fiber tracts, we conducted partial least square (PLS) regression (Abdi, 2010). Because of the high variability in some of the tractography measurements, all tractography measurements were transformed into ranks before further processing. To test the generalization of the result to a new dataset, the jackknife procedure (a.k.a 'leave one out') of PLS regression was performed by taking out participants one by one and predicting their neuropsychological test scores using the remaining participants. The quality of the prediction was evaluated using Pearson's correlation coefficient between the working memory scores and predicted scores.

The PLS regression was conducted using Matlab scripts. For multiple regression, the Matlab function, regstats, was utilized. The Benjamini-Hochberg method of false discovery rate (FDR) (Benjamini and Hochberg, 1995) implemented in the Matlab function, FDR, was applied to control for family-wise error for each type of analyses (e.g. the correlation between tractography measurements and *FMR1*-related measurements was considered as one type of the analyses, so FDR was applied to all tractography and *FMR1*-related measurements).

RESULTS

Research participants

Thirty-seven healthy males were recruited (age mean ± SD = 40.7 ± 17.3 years; range, 18–80 years) who served as the comparison group for studies investigating the effect of *FMR1* premutation on brain and behavior (Table 1). CGG length of these participants ranged from 19 to 42. The average mRNA level was 1.48 (SD 0.26). The average FMRP level was 109.7 (SD 56.1) for the 32 males whose FMRP levels were available. One male's FMRP level (29-years-old) was 473.6, about 6.5 SD higher than the group average. This value was treated as an outlier and excluded from all analyses involving FMRP. Working memory performance

$watermark-text $watermark-text $watermark-text

$watermark-text

$watermark-text

$watermark-text

was evaluated using Working Memory Index from Wechsler Memory Scale, Third Edition (WMS-III) (Wechsler, 1997b). The score for one 24-year-old male was 71, about 2.8 SD lower than the group mean (112, SD 15). As a result, this score was excluded from further analysis.

Effect of FMR1 gene expression on tractography measurements

We acquired DTI from 32 male controls and performed tractography (Catani et al., 2005; Mori et al., 1999; Wakana et al., 2004) to reconstruct fiber tracts important for working memory; namely, arcuate fasciculus complex, anterior cingulum, inferior longitudinal fasciculus (ILF), and genu (CCg) and anterior body (CCab) of the corpus callosum (Fig. 1). Of these 32 males, 27 had available FMRP data. While no tractography measurements showed correlation with *FMR1* CGG-repeat length, 13 measurements passed 5% FDR ($p = 0.013$) showing correlation with *FMR1* mRNA and/or FMRP after age-adjustment. The measurements that exhibited significant correlation with *FMR1* mRNA were FA and MD of left arcuate fasciculus and left ILF, and FA of right ILF, CCg, and CCab. Five measurements showed significant correlation with FMRP: tract volume of bilateral ILF and CCab, and FA of left ILF and CCg (Table 2). *FMR1* mRNA reduction and FMRP elevation were uniformly associated with elevation in FA and tract volume, and reduction in MD.

We further tested the unique effect of the *FMR1* mRNA and FMRP on tractography measurements using mRNA, FMRP, and age as independent variables in multiple regression. Five tractography measurements continued to show significant correlation with *FMR1* mRNA in 32 males: the FA (partial $r^2 = 0.22$, $p = 0.019$) and MD (partial $r^2 = 0.20$, $p = 0.023$) of left arcuate fasciculus, FA (partial $r^2 = 0.24$, $p = 0.013$) and MD (partial $r^2 = 0.25$, $p = 0.010$) of left ILF, and FA (partial $r^2 = 0.17$, $p = 0.044$) of right ILF. Four measurements continued to display significant correlation with FMRP in the 27 males: the tract volume of left (partial $r^2 = 0.34$, $p = 0.008$) and right (partial $r^2 = 0.28$, $p = 0.016$) ILF, CCg FA (partial $r^2 = 0.31$, $p = 0.049$), and CCab tract volume (partial $r^2 = 0.15$, $p = 0.039$).

As 14/32 participants had a past mood and/or anxiety disorder, we added SCID diagnosis as an additional covariate in the multiple linear regression using age and *FMR1* variables for predicting tractography measurements. SCID diagnosis was not significant for any of the predictions. Tractography measurements correlated significant with *FMR1* mRNA at 5% FDR ($p = 0.006$) were left AFc FA and MD, left ILF FA and MD, and CCab FA. In addition, tract volume of bilateral ILF correlated significantly with FMRP.

Effect of FMR1 mRNA and FMRP on voxel-based DTI measurements

To examine the correlation between the *FMR1* mRNA and FMRP and white matter integrity without *a priori* assumptions, we conducted voxel-based analysis at the white matter core using tract-based spatial statistics(Smith et al., 2006) (TBSS). Using age as a covariate, TBSS revealed widespread positive correlations between FMRP and FA (Fig. 2a) most prominent at rostral white matter regions, impacting the frontal white matter, extreme capsule, internal capsule, arcuate fasciculus, ILF, cingulum, and corpus callosum. TBSS also showed significant negative correlations between *FMR1* mRNA level and FA in a broad distribution of cerebral white matter, with only the fornix body and cerebellar peduncles not showing this correlation (Fig. 2b). TBSS showed positive correlations between *FMR1* mRNA and MD in the CCg, arcuate fasciculus, and ILF (Fig. 2c). Subsequently, TBSS analyses were performed on axial diffusivity (AD) (i.e. the amount of diffusion along the predominant diffusion direction) and radial diffusivity (RD) (i.e. the average diffusion perpendicular to the predominant diffusion direction) maps to discern which DTI parameter contributed to the association between *FMR1* mRNA and MD (Song et al., 2002). The result

demonstrated wide-spread association between *FMR1* mRNA and RD similar to the association between *FMR1* mRNA and FA (Fig. 2d).

Effect of FMR1 gene expression on global brain measurements

We further investigated the relationship of *FMR1* mRNA and FMRP with whole brain measurements such as gray and white matter volume, the average FA of the white matter, and the average MD of the gray and white matter (Table 3). The gray matter volume survived 5% FDR ($p = 0.015$), showing significant correlation with FMRP after controlling for age (Fig. 3b). As the younger and older participants were scanned using two different T1-weighted sequences, we further analyzed the data involving the volume estimations from Sienax (i.e. gray and white matter volumes) using scanner as an additional covariate. The addition of the scanner covariate made only negligible changes to the prediction of the gray matter volumes from FMRP, and the scanner was not a substantial contributor to the associations (Appendix Table 1).

Associations between brain measurements and working memory

Next, we assessed the associations of brain measurements with working memory performance. Twelve tractography measurements passed 5% FDR ($p = 0.011$) after excluding the age effect (Appendix Table 2). All FA and MD measurements showed significant correlation except the FA of right arcuate fasciculus, MD of left ILF, and FA and MD of CCg. In addition, the FA measurements uniformly exhibited positive correlation with working memory performance while the MD measurements exhibited negative correlation. For the association between global brain measurements and working memory performance, white matter FA ($n = 27$, partial $r^2 = 0.26$, $p = 0.007$) and MD ($n = 27$, partial $r^2 = 0.33$, $p = 0.002$) reached significance at 5% FDR ($p = 0.007$).

To test whether the combination of the 24 tractography measurements could predict working memory performance, we conducted partial least square (PLS) regression (Abdi, 2010) to find the latent variables that explain the most covariance between the tractography measurements and working memory scores. We also applied the jackknife procedure (a.k.a leave-one-out) to test the generalizability of the results to new datasets. The tractography measurements were able to predict working memory significantly ($n = 27$, $r = 0.73$, $p < 0.001$; jackknife $r = 0.65$, $p < 0.001$). Only one latent variable was identified from the PLS regression, which explained 46.2% variance of the tractography measurements and 53.4% variance of the working memory score. The analysis of the latent variables showed 21/24 measurements made substantial contribution to the prediction. The exceptions were the tract volume of left AFc, left cingulum and right ILF.

Association between FMR1 gene expression and working memory

FMR1 CGG repeat length, mRNA, and protein show neither a correlation with age, nor with each other. In contrast, the scores of working memory showed a negative correlation with *FMR1* mRNA ($r = -0.37$, $p = 0.039$) and the positive correlation with FMRP approached significance ($r = 0.35$, $p = 0.064$) (Fig. 4).

Associations with T2-hyperintensive lesions

As the amount of T2-hyperintensive lesions may be an important contributing factor in older participants, we further studied correlation between T2-hyperintensive lesions with all measurements obtained in the current study (age, tractography measurements, global brain measurements, CGG repeat size, *FMR1* mRNA, FMRP, and working memory performance) in the 13 males above age 50. We counted number of brain areas with T2-hyperintensive lesions in the areas of the cerebellar peduncles, pons, corpus callosum, bilateral insula, and

$watermark-text $watermark-text $watermark-text

bilateral frontal, parietal, and temporal lobes. The results showed that the average number of brain areas with T2-hyperintensive lesions was 2.3, SD 1.7, range 0–5. No measurements showed significant correlation at 5% or even 10% FDR. We concluded that T2-hyperintensive lesions probably do not have a major effect on our main findings.

DISCUSSION

Accumulating evidence from molecular studies suggests the involvement of *FMR1* at both preand post-synaptic sites for shaping brain circuits critical for cognitive processing (Bassell and Warren, 2008). We present structural imaging findings consistent with these observations, showing significant associations in healthy males between *FMR1* transcriptional and translational expression and white matter structural organization, and between FMRP and gray matter volume. These findings indicate the role of *FMR1* gene expression in modulating brain structures that is observable even within the normal *FMR1* CGG-repeat range. While the structural connectivity analyses revealed positive associations of FMRP with the structural organization of the ILF, CCg, and CCab, voxel-based analysis using TBSS detected widespread positive association with FA in rostral white matter regions, impacting the frontal white matter, extreme capsule, internal capsule, arcuate fasciculus, ILF, cingulum, and corpus callosum. The association of *FMR1* mRNA with white matter structural organization was even more widespread compared to that of FMRP, being apparent in six major fiber tracts (the cerebral peduncular fibers, extreme capsule fibers, arcuate fasciculus, ILF, cingulum, and corpus callosum) in DTI tractography and voxel-based TBSS analyses.

Although the broadly-distributed effect of FMRP and *FMR1* mRNA were unexpected in the normal population, the findings are consistent with the gene's role in translation regulation of one-third of the proteins in the pre- and post-synaptic proteome critical for synaptic plasticity (Darnell et al., 2011). One of these proteins is the myelin basic protein (MBP), which is an essential protein component of the myelin sheath (Kamholz et al., 1987) and a prominent constituent of intranuclear inclusions in premutation carriers with FXTAS who present with widespread myelin and axonal damage in the CNS (Greco et al., 2006). Through the control of synthesis and RNA-stability of MBP and other synaptic proteins (Wang et al., 2004; Zalfa et al., 2007), the *FMR1* may be a part of the signal transduction pathways converting receptor activity into physiological changes in brain structures (Darnell et al., 2011).

In this study, we explored the mechanism through which *FMR1* expression may influence white matter structures. We compared voxel-based AD and RD values in TBSS to discern whether the amount of myelination played a role in the association. The rationale for this investigation was derived from the shiverer mouse model of dysmyelination in which homozygous recessive autosomal mutation of MBP leads to incomplete myelin formation in the CNS. Importantly, the dysmyelination in the shiverer mice manifested in DTI as RD elevation without changes in AD (Song et al., 2002). We found RD, not AD, showed significant positive association with *FMR1* mRNA. In healthy conditions, both more fiber branching and less myelination can lead to RD elevation. However, theoretically if all other conditions (e.g. tissue packing density, myelination, etc.) are held constant, fiber branching alone does not affect MD, which is determined by the amount of restrictions to water diffusion due to the presence of biological tissues (Basser and Pierpaoli, 1996); in contrast, reduced myelination can lead to increased MD due to the RD elevation (Beaulieu, 2002). In the current study, both TBSS and tractography analyses detected the associations of higher *FMR1* mRNA with FA reduction and MD elevation in the same areas. Therefore, less myelination was more likely than fiber branching to be the major contributor to the

$watermark-text $watermark-text $watermark-text

$watermark-text

$watermark-text

$watermark-text

increased RD associated with elevated mRNA. Further verifications are needed to test this assumption.

It is important to note that the current study presents indirect measurements of *FMR1* and FMRP expressions in the brain and white matter structural organization. In particular, the levels of *FMR1* mRNA and FMRP were measured from peripheral blood lymphocytes and therefore are not brain area-specific, and the white matter structural organization was inferred through brain imaging. Although critical, it is unknown whether our findings reflect the true associations between *FMR1* and FMRP expressions and white matter structural organization in specific brain areas. In addition, the direction of correlation between *FMR1* and FMRP expressions and brain measurements needs to be verified through larger studies, although the current observations are consistent with the existing evidence. FMRP levels showed a positive correlation with gray matter volume and the volume and FA of fiber tracts in the current study. Although speculative, it is possible that increased (FMRP-dependent) translocation of MBP mRNA to the myelin compartment is partially responsible for the observed positive correlation between FMRP and FA. The direction of correlation is also in line with the finding from fragile X full mutation. In fragile X full mutation, lack of FMRP expression lead to immature dendritic spine and axon morphology (Irwin et al., 2001; Tessier and Broadie, 2008) and arrested growth of white matter volume during adolescence (Bray et al., 2011). Elevated cortical and subcortical volumes have been observed in boys with fragile X syndrome, which is postulated to be caused by insufficient pruning due to FMRP depletion (Hoeft et al., 2010; Meguid et al., 2012). However, this does not preclude that the insufficient pruning during development may lead to an accelerated decline in gray matter volume at adulthood seen in individuals with autism (Courchesne et al., 2011). Consistently, in adult males with fragile X syndrome (mean age 30 years, SD 8 years), no differences in gray matter volumes were detected compared to age-matched controls, although both regional volume elevation and reduction were present (Hallahan et al., 2011). For white matter FA and MD, no significant correlation with *FMR1* mRNA or FMRP has been reported in fragile X premutation or full mutation, although reduced FA in the frontostriatal pathway and parietal sensory-motor areas relative to healthy controls has been found in female full mutation carries (age 13.1–22.7 years) (Barnea-Goraly et al., 2003). When comparing premutation carriers without FXTAS to age-match controls, we detected significant diffusivity elevation in the middle cerebellar peduncle and left cerebral peduncle in older carriers (> 40 years old) (Hashimoto et al., 2011b) and greater age-related decline of FA in the extreme capsule (Wang et al., 2012b) in young carriers (< 45 years old). Additional studies are needed to further delineate the complex trajectory of brain volume changes over the life span in relation to individual differences in FMRP expression levels in normal alleles and to establish the influence of dendritic spine morphology on gray matter volume and white matter structures in normal, premutation, and full mutation alleles.

The current study also showed negative correlation between *FMR1* mRNA and white matter structural organization, suggesting that higher levels of *FMR1* mRNA may exert a subtle (i.e., sub-clinical) “toxic” influence on cellular function, or may possibly prevent FMRP from functioning optimally. However, this “toxic” influence on cellular function in normal alleles may be fundamentally distinct from the RNA-toxicity gain of function effect observed in premutation alleles (Garcia-Arocena and Hagerman, 2010; Hagerman, 2012; Hagerman and Hagerman, 2004), which requires both long, expanded CGG repeats in the premutation range and elevated *FMR1* mRNA levels for sequential sequestration of proteins vital for cell survival into giant RNA aggregates (Hoem et al., 2011; Sellier et al., 2010). In addition, *FMR1* transcriptional level may be modulated in different ways between premutation and normal alleles. Both *cis* and *trans* regulatory elements and epigenetic modifications have been identified to influence *FMR1* mRNA level. These are the signaling pathways involved in retinoic acid, Ca^{2+}, neuronal activity, and cellular stress, histone

$watermark-text

$watermark-text

$watermark-text

modification, and proteins that bind to *FMR1* promoter (Bear et al., 2004; Jeon et al., 2011; Lim et al., 2005; Pfeiffer et al., 2010). In premutation alleles, *FMR1* mRNA and FMRP expression levels may be particularly influenced by the CGG repeat element in the 5' untranslated region, evident by the positive correlation between *FMR1* mRNA and CGG repeat length and the negative correlation between FMRP and CGG repeat length (Tassone et al., 2007a; Tassone et al., 2000). While the abnormal regulation of 5'- and 3'-untranslated regions (UTRs), due to CGG expansion, may underlie the slight FMRP-deficiency in fragile X premutation (Beilina et al., 2004; Tassone et al., 2011), the mechanisms through which the CGG element exerts an influence on the transcript level remain elusive. In normal alleles, the associations between CGG repeat length and levels of *FMR1* transcript and protein do not exist (Tassone et al., 2007b) probably due to the absence of the regulatory effect from the *cis* elements. Therefore, we did not expect to find a strong correlation between *FMR1* mRNA and brain structures in normal alleles. Important aims for future studies are to conduct histological and animal studies to verify the associations between *FMR1* gene and brain structures and to shed light on the specific cellular mechanisms underlying the influence from *FMR1* gene.

The analyses of gene-brain-behavior relationships demonstrated the functional significance of both *FMR1* gene expression and tractography measurements. While *FMR1* mRNA levels showed weak, but significant correlation with working memory performance, the four working memory-related fiber tracts demonstrated robust correlation with working memory performance except for the CCg, which showed correlation significant at 10% FDR. Importantly, the correlation between the fiber tracts and working memory performance are highly generalizable to new datasets as it is indicated by the jackknife procedure of PLS regression. The four fiber tracts provide structural backbones for a distributed neural network of working memory, interconnecting posterior parietal cortex important for spatial processing, prefrontal lobe for higher level cognitive control and maintenance, occipito-temporal areas for object recognition, and anterior cingulate gyrus for attention (Zimmer, 2008). The involvement of the arcuate fasciculus and CCab in working memory is consistent with the recent findings of increased FA in these two fiber regions as the result of working memory training (Takeuchi et al., 2010). The widespread correlation between white matter fiber tracts and working memory is also in concordance with a recent study of 420 adults between age 70–80 years (Penke et al., 2012) in which the latent FA factor from 12 major fiber tracts correlated strongly with general intelligence. It is possible (and likely) that the *FMR1* plays a role in other aspects of cognition that we did not include in the analyses. In addition, an inheritance study has suggested the presence of potential common genetic factors that contribute to both working memory and the FA of superior longitudinal fasciculus (contains the anterior arcuate fasciculus and the arcuate fasciculus) (Karlsgodt et al., 2010). The current study suggests the *FMR1* as a potential candidate for a genetic factor common to both brain structural connectivity and working memory if the correlation between the *FMR1* and working memory can be verified in a larger study. Alternatively, the *FMR1* may exert its effect on working memory through the brain, indicated by the strong correlation of the brain measurements with both *FMR1* and FMRP expressions and working memory performance. This finding is significant given the role of working memory as a central component of human intelligence (Wechsler, 1997a). Understanding the cellular mechanisms underlying these relationships may help us discover effective treatments for disorders associated with fragile X premutation and full mutation.

One strength of the current study was to utilize multiple imaging analysis methods (i.e. DTI tractography- and voxel-based measurements and brain-level DTI and volume measurements), and statistical tools (i.e. multiple linear regression and PLS regression) to verify the results and showed general consistency of the findings. The verification using multiple methods is important since the associations between *FMR1* mRNA and brain

$watermark-text

$watermark-text

$watermark-text

structures were unexpected in normal alleles based on the small range of *FMR1* mRNA levels. Nevertheless, readers should consider the findings with certain caveats. As mentioned above, the obtained *FMR1* mRNA and FMRP levels, and white matter structural organization, were indirect measurements of the brain values and thus require verifications from histological and animal studies. The anterior arcuate fasciculus overlaps with the SLFIII (Thiebaut de Schotten et al., 2012). However, other branches of SLF (i.e. SLFI and SLFII) that have shown importance for working memory cannot be reconstructed using the current method. Utilizing cortical-area-based ROIs may be advantageous over ROI-drawings on coronal or sagittal slices for the successful reconstruction of the SLF. Limitations in DTI image acquisition and preprocessing included relatively low *b*-value (700 s/mm^2), uncorrected partial volume effect from CSF and EPI distortion, and insufficient control over subject motion and cardiac pulsation. These might have added noise to DTI measurements especially in the areas around the lateral ventricles, brain stem, cerebellum, and prefrontal lobes (Huang et al., 2008; Irfanoglu et al., 2012; Jones and Cercignani, 2010; Pasternak et al., 2009; Tournier et al., 2011). In the current study, we used archival DTI data acquired during 2007–2009, and parallel imaging was not available for these image acquisitions. The amount of EPI distortion may be too severe to be corrected effectively using post-processing techniques (Huang et al., 2008). We are currently collecting DTI with parallel imaging along with T2-weighted MRI, which will allow the application of post-processing methods for correcting EPI-distortion (Huang et al., 2008; Irfanoglu et al., 2012). These images will be useful for verifying the results in the current manuscript, although we do not yet have an adequate number of scans to perform the analysis. We selected fiber tracts having a major role in working memory or having working memory as their primary function in the study. The current list is not exhaustive, and thus might have excluded other fiber tracts important for working memory. Although the effect of *FMR1* gene on the brain is robust, the sample size is relatively small comparing to other genetic studies. The sample is not entirely healthy as revealed by the SCID and hypertension and diabetes review. Future studies could examine the effect of *FMR1* in healthy controls without these issues and in patients with anxiety and mood disorders, hypertension, and diabetes in details. In addition, it remains unknown whether the observed effect of *FMR1* expression on brain structures and working memory extends to other populations such as females, or children whose brains are still developing under the influence from *FMR1* and other genes.

CONCLUSIONS

The current study revealed a novel finding of *FMR1* as a potential common genetic factor underlying individual differences in brain structure and working memory in healthy males. *FMR1* mRNA exhibited significant correlation with working memory, and the fiber tracts important for working memory displayed significant associations with both *FMR1* and working memory performance. Further studies are needed to elucidate cellular mechanisms underpinning the influence of *FMR1* on brain structure.

Supplementary Material

Refer to Web version on PubMed Central for supplementary material.

Acknowledgments

We are grateful to the research participants and their families; to Vivien Narcissa, Cindy Johnston, and Floridette Abucayan for participant recruitment; to John Wang and Patrick Adams for image and data collection; Jenny Tram and John Shell for performing fiber tracking; Danielle Harvey for statistical support; and Pamela Gallego for editorial comments. This project was supported by NIH grants HD036071, HD02274, MH078041, MH077554, NS062412, UL1DE019583, RL1AG032119, RL1AG032115, and TL1DA024854.

$watermark-text

$watermark-text

$watermark-text

REFERENCES

Abdi H. Partial least squares regression and projection on latent structure regression (PLS-Regression). Wiley Interdisciplinary Reviews: Computational Statistics. 2010; 2:97–106.

Baddeley A. The episodic buffer: a new component of working memory? Trends Cogn Sci. 2000; 4:417–423. [PubMed: 11058819]

Barnea-Goraly N, Eliez S, Hedeus M, Menon V, White CD, Moseley M, Reiss AL. White matter tract alterations in fragile X syndrome: preliminary evidence from diffusion tensor imaging. Am J Med Genet B Neuropsychiatr Genet. 2003; 118B:81–88. [PubMed: 12627472]

Bassell GJ, Warren ST. Fragile X syndrome: loss of local mRNA regulation alters synaptic development and function. Neuron. 2008; 60:201–214. [PubMed: 18957214]

Basser PJ, Pierpaoli C. Microstructural and physiological features of tissues elucidated by quantitative-diffusion-tensor MRI. J. Magn. Reson. B. 1996; 111:209–219. [PubMed: 8661285]

Bear MF, Huber KM, Warren ST. The mGluR theory of fragile X mental retardation. Trends Neurosci. 2004; 27:370–377. [PubMed: 15219735]

Beaulieu C. The basis of anisotropic water diffusion in the nervous system - a technical review. NMR Biomed. 2002; 15:435–455. [PubMed: 12489094]

Beilina A, Tassone F, Schwartz PH, Sahota P, Hagerman PJ. Redistribution of transcription start sites within the FMR1 promoter region with expansion of the downstream CGG-repeat element. Hum Mol Genet. 2004; 13:543–549. [PubMed: 14722156]

Benjamini Y, Hochberg Y. Controlling the False Discovery Rate - a Practical and Powerful Approach to Multiple Testing. J. R. Statist. Soc. B. 1995; 57:289–300.

Bray S, Hirt M, Jo B, Hall SS, Lightbody AA, Walter E, Chen K, Patnaik S, Reiss AL. Aberrant frontal lobe maturation in adolescents with fragile X syndrome is related to delayed cognitive maturation. Biol Psychiatry. 2011; 70:852–858. [PubMed: 21802660]

Burzynska AZ, Nagel IE, Preuschhof C, Li SC, Lindenberger U, Backman L, Heekeren HR. Microstructure of frontoparietal connections predicts cortical responsivity and working memory performance. Cereb Cortex. 2011; 21:2261–2271. [PubMed: 21350048]

Catani M, Jones DK, ffytche DH. Perisylvian language networks of the human brain. Ann Neurol. 2005; 57:8–16. [PubMed: 15597383]

Charlton RA, Barrick TR, Lawes IN, Markus HS, Morris RG. White matter pathways associated with working memory in normal aging. Cortex. 2010; 46:474–489. [PubMed: 19666169]

Chen Y, Tassone F, Berman RF, Hagerman PJ, Hagerman RJ, Willemsen R, Pessah IN. Murine hippocampal neurons expressing Fmr1 gene premutations show early developmental deficits and late degeneration. Hum Mol Genet. 2010; 19:196–208. [PubMed: 19846466]

Chonchaiya W, Au J, Schneider A, Hessl D, Harris SW, Laird M, Mu Y, Tassone F, Nguyen DV, Hagerman RJ. Increased prevalence of seizures in boys who were probands with the FMR1 premutation and co-morbid autism spectrum disorder. Hum Genet. 2011

Cornish KM, Kogan CS, Li L, Turk J, Jacquemont S, Hagerman RJ. Lifespan changes in working memory in fragile X premutation males. Brain Cogn. 2009; 69:551–558. [PubMed: 19114290]

Courchesne E, Campbell K, Solso S. Brain growth across the life span in autism: age-specific changes in anatomical pathology. Brain Res. 2011; 1380:138–145. [PubMed: 20920490]

Crawford DC, Meadows KL, Newman JL, Taft LF, Pettay DL, Gold LB, Hersey SJ, Hinkle EF, Stanfield ML, Holmgreen P, Yeargin-Allsopp M, Boyle C, Sherman SL. Prevalence and phenotype consequence of FRAXA and FRAXE alleles in a large, ethnically diverse, special education-needs population. Am J Hum Genet. 1999; 64:495–507. [PubMed: 9973286]

Cunningham CL, Martinez Cerdeno V, Navarro Porras E, Prakash AN, Angelastro JM, Willemsen R, Hagerman PJ, Pessah IN, Berman RF, Noctor SC. Premutation CGG-repeat expansion of the Fmr1 gene impairs mouse neocortical development. Hum Mol Genet. 2011; 20:64–79. [PubMed: 20935171]

Darnell JC, Van Driesche SJ, Zhang C, Hung KY, Mele A, Fraser CE, Stone EF, Chen C, Fak JJ, Chi SW, Licatalosi DD, Richter JD, Darnell RB. FMRP stalls ribosomal translocation on mRNAs linked to synaptic function and autism. Cell. 2011; 146:247–261. [PubMed: 21784246]

$watermark-text

Devys D, Lutz Y, Rouyer N, Bellocq JP, Mandel JL. The FMR-1 protein is cytoplasmic, most abundant in neurons and appears normal in carriers of a fragile X premutation. Nat Genet. 1993; 4:335–340. [PubMed: 8401578]

Farzin F, Perry H, Hessl D, Loesch D, Cohen J, Bacalman S, Gane L, Tassone F, Hagerman P, Hagerman R. Autism spectrum disorders and attention-deficit/hyperactivity disorder in boys with the fragile X premutation. J Dev Behav Pediatr. 2006; 27:S137–S144. [PubMed: 16685180]

Filipovic-Sadic S, Sah S, Chen L, Krosting J, Sekinger E, Zhang W, Hagerman PJ, Stenzel TT, Hadd AG, Latham GJ, Tassone F. A novel FMR1 PCR method for the routine detection of low abundance expanded alleles and full mutations in fragile X syndrome. Clin Chem. 2010; 56:399–408. [PubMed: 20056738]

Garcia-Arocena D, Hagerman PJ. Advances in understanding the molecular basis of FXTAS. Hum Mol Genet. 2010; 19:R83–R89. [PubMed: 20430935]

Greco CM, Berman RF, Martin RM, Tassone F, Schwartz PH, Chang A, Trapp BD, Iwahashi C, Brunberg J, Grigsby J, Hessl D, Becker EJ, Papazian J, Leehey MA, Hagerman RJ, Hagerman PJ. Neuropathology of fragile X-associated tremor/ataxia syndrome (FXTAS). Brain. 2006; 129:243–255. [PubMed: 16332642]

Greene CM, Braet W, Johnson KA, Bellgrove MA. Imaging the genetics of executive function. Biol Psychol. 2008; 79:30–42. [PubMed: 18178303]

Hagerman PJ. Current gaps in understanding the molecular basis of FXTAS. Tremor Other Hyperkinet Mov 2. 2012 http://tremorjournal.org/article/view/63.

Hagerman PJ, Hagerman RJ. The fragile-X premutation: a maturing perspective. Am J Hum Genet. 2004; 74:805–816. [PubMed: 15052536]

Hallahan BP, Craig MC, Toal F, Daly EM, Moore CJ, Ambikapathy A, Robertson D, Murphy KC, Murphy DG. In vivo brain anatomy of adult males with Fragile X syndrome: an MRI study. Neuroimage. 2011; 54:16–24. [PubMed: 20708694]

Hashimoto R, Backer KC, Tassone F, Hagerman RJ, Rivera SM. An fMRI study of the prefrontal activity during the performance of a working memory task in premutation carriers of the fragile X mental retardation 1 gene with and without fragile X-associated tremor/ataxia syndrome (FXTAS). J Psychiatr Res. 2011a; 45:36–43. [PubMed: 20537351]

Hashimoto R, Srivastava S, Tassone F, Hagerman RJ, Rivera SM. Diffusion tensor imaging in male premutation carriers of the fragile X mental retardation gene. Mov Disord. 2011b; 26:1329–1336. [PubMed: 21484870]

Hoeft F, Carter JC, Lightbody AA, Cody Hazlett H, Piven J, Reiss AL. Region-specific alterations in brain development in one- to three-year-old boys with fragile X syndrome. Proc Natl Acad Sci U S A. 2010; 107:9335–9339. [PubMed: 20439717]

Hoem G, Raske CR, Garcia-Arocena D, Tassone F, Sanchez E, Ludwig AL, Iwahashi CK, Kumar M, Yang JE, Hagerman PJ. CGG-repeat length threshold for FMR1 RNA pathogenesis in a cellular model for FXTAS. Hum Mol Genet. 2011; 20:2161–2170. [PubMed: 21389081]

Huang H, Ceritoglu C, Li X, Qiu A, Miller MI, van Zijl PC, Mori S. Correction of B0 susceptibility induced distortion in diffusion-weighted images using large-deformation diffeomorphic metric mapping. Magn Reson Imaging. 2008; 26:1294–1302. [PubMed: 18499384]

Irfanoglu MO, Walker L, Sarlls J, Marenco S, Pierpaoli C. Effects of image distortions originating from susceptibility variations and concomitant fields on diffusion MRI tractography results. Neuroimage. 2012; 61:275–288. [PubMed: 22401760]

Irwin SA, Patel B, Idupulapati M, Harris JB, Crisostomo RA, Larsen BP, Kooy F, Willems PJ, Cras P, Kozlowski PB, Swain RA, Weiler IJ, Greenough WT. Abnormal dendritic spine characteristics in the temporal and visual cortices of patients with fragile-X syndrome: a quantitative examination. Am J Med Genet. 2001; 98:161–167. [PubMed: 11223852]

Iwahashi C, Tassone F, Hagerman RJ, Yasui D, Parrott G, Nguyen D, Mayeur G, Hagerman PJ. A quantitative ELISA assay for the fragile×mental retardation 1 protein. J Mol Diagn. 2009; 11:281–289. [PubMed: 19460937]

Jeon SJ, Seo JE, Yang SI, Choi JW, Wells D, Shin CY, Ko KH. Cellular stress-induced up-regulation of FMRP promotes cell survival by modulating PI3K-Akt phosphorylation cascades. J Biomed Sci. 2011; 18:17. [PubMed: 21314987]

$watermark-text

Jones DK, Cercignani M. Twenty-five pitfalls in the analysis of diffusion MRI data. NMR Biomed. 2010; 23:803–820. [PubMed: 20886566]

Kamholz J, Spielman R, Gogolin K, Modi W, O'Brien S, Lazzarini R. The human myelin-basic-protein gene: chromosomal localization and RFLP analysis. Am J Hum Genet. 1987; 40:365–373. [PubMed: 2437795]

Karlsgodt KH, Bachman P, Winkler AM, Bearden CE, Glahn DC. Genetic influence on the working memory circuitry: Behavior, structure, function and extensions to illness. Behav Brain Res. 2011; 225:610–622. [PubMed: 21878355]

Karlsgodt KH, Kochunov P, Winkler AM, Laird AR, Almasy L, Duggirala R, Olvera RL, Fox PT, Blangero J, Glahn DC. A multimodal assessment of the genetic control over working memory. J Neurosci. 2010; 30:8197–8202. [PubMed: 20554870]

Lanfranchi S, Cornoldi C, Drigo S, Vianello R. Working memory in individuals with fragile X syndrome. Child Neuropsychol. 2009; 15:105–119. [PubMed: 18608221]

Lim JH, Booker AB, Fallon JR. Regulating fragile X gene transcription in the brain and beyond. J Cell Physiol. 2005; 205:170–175. [PubMed: 15895397]

Meguid NA, Fahim C, Sami R, Nashaat NH, Yoon U, Anwar M, El-Dessouky HM, Shahine EA, Ibrahim AS, Mancini-Marie A, Evans AC. Cognition and lobar morphology in full mutation boys with fragile X syndrome. Brain Cogn. 2012; 78:74–84. [PubMed: 22070923]

Mori S, Crain BJ, Chacko VP, van Zijl PC. Three-dimensional tracking of axonal projections in the brain by magnetic resonance imaging. Ann. Neurol. 1999; 45:265–269. [PubMed: 9989633]

Oostra BA, Willemsen R. FMR1: a gene with three faces. Biochim Biophys Acta. 2009; 1790:467–477. [PubMed: 19233246]

Pasternak O, Sochen N, Gur Y, Intrator N, Assaf Y. Free water elimination and mapping from diffusion MRI. Magn Reson Med. 2009; 62:717–730. [PubMed: 19623619]

Penke L, Maniega SM, Bastin ME, Valdes Hernandez MC, Murray C, Royle NA, Starr JM, Wardlaw JM, Deary IJ. Brain white matter tract integrity as a neural foundation for general intelligence. Mol Psychiatry. 2012

Pfeiffer BE, Zang T, Wilkerson JR, Taniguchi M, Maksimova MA, Smith LN, Cowan CW, Huber KM. Fragile X mental retardation protein is required for synapse elimination by the activity-dependent transcription factor MEF2. Neuron. 2010; 66:191–197. [PubMed: 20434996]

Pieretti M, Zhang FP, Fu YH, Warren ST, Oostra BA, Caskey CT, Nelson DL. Absence of expression of the FMR-1 gene in fragile X syndrome. Cell. 1991; 66:817–822. [PubMed: 1878973]

Rama P. Domain-dependent activation during spatial and nonspatial auditory working memory. Cogn Process. 2008; 9:29–34. [PubMed: 17885775]

Sellier C, Rau F, Liu Y, Tassone F, Hukema RK, Gattoni R, Schneider A, Richard S, Willemsen R, Elliott DJ, Hagerman PJ, Charlet-Berguerand N. Sam68 sequestration and partial loss of function are associated with splicing alterations in FXTAS patients. EMBO J. 2010; 29:1248–1261. [PubMed: 20186122]

Sepulcre J, Masdeu JC, Pastor MA, Goni J, Barbosa C, Bejarano B, Villoslada P. Brain pathways of verbal working memory: a lesion-function correlation study. Neuroimage. 2009; 47:773–778. [PubMed: 19393745]

Smith SM. Fast robust automated brain extraction. Hum Brain Mapp. 2002; 17:143–155. [PubMed: 12391568]

Smith SM, Jenkinson M, Johansen-Berg H, Rueckert D, Nichols TE, Mackay CE, Watkins KE, Ciccarelli O, Cader MZ, Matthews PM, Behrens TE. Tract-based spatial statistics: voxelwise analysis of multi-subject diffusion data. Neuroimage. 2006; 31:1487–1505. [PubMed: 16624579]

Smith SM, Zhang Y, Jenkinson M, Chen J, Matthews PM, Federico A, De Stefano N. Accurate, robust, and automated longitudinal and cross-sectional brain change analysis. Neuroimage. 2002; 17:479–489. [PubMed: 12482100]

Song SK, Sun SW, Ramsbottom MJ, Chang C, Russell J, Cross AH. Dysmyelination revealed through MRI as increased radial (but unchanged axial) diffusion of water. Neuroimage. 2002; 17:1429–1436. [PubMed: 12414282]

$watermark-text

Takeuchi H, Sekiguchi A, Taki Y, Yokoyama S, Yomogida Y, Komuro N, Yamanouchi T, Suzuki S, Kawashima R. Training of working memory impacts structural connectivity. J Neurosci. 2010; 30:3297–3303. [PubMed: 20203189]

Tassone F, Adams J, Berry-Kravis EM, Cohen SS, Brusco A, Leehey MA, Li L, Hagerman RJ, Hagerman PJ. CGG repeat length correlates with age of onset of motor signs of the fragile X-associated tremor/ataxia syndrome (FXTAS). Am J Med Genet B Neuropsychiatr Genet. 2007a; 144B:566–569. [PubMed: 17427188]

Tassone F, Beilina A, Carosi C, Albertosi S, Bagni C, Li L, Glover K, Bentley D, Hagerman PJ. Elevated FMR1 mRNA in premutation carriers is due to increased transcription. RNA. 2007b; 13:555–562. [PubMed: 17283214]

Tassone F, De Rubeis S, Carosi C, La Fata G, Serpa G, Raske C, Willemsen R, Hagerman PJ, Bagni C. Differential usage of transcriptional start sites and polyadenylation sites in FMR1 premutation alleles. Nucleic Acids Res. 2011; 39:6172–6185. [PubMed: 21478165]

Tassone F, Hagerman RJ, Taylor AK, Gane LW, Godfrey TE, Hagerman PJ. Elevated levels of *FMR1* mRNA in carrier males: a new mechanism of involvement in the fragile-X syndrome. Am J Hum Genet. 2000; 66:6–15. [PubMed: 10631132]

Tessier CR, Broadie K. Drosophila fragile X mental retardation protein developmentally regulates activity-dependent axon pruning. Development. 2008; 135:1547–1557. [PubMed: 18321984]

Thiebaut de Schotten M, Dell'Acqua F, Forkel SJ, Simmons A, Vergani F, Murphy DG, Catani M. A lateralized brain network for visuospatial attention. Nat Neurosci. 2012; 14:1245–1246. [PubMed: 21926985]

Tournier JD, Mori S, Leemans A. Diffusion tensor imaging and beyond. Magn Reson Med. 2011; 65:1532–1556. [PubMed: 21469191]

Verkerk AJ, Pieretti M, Sutcliffe JS, Fu YH, Kuhl DP, Pizzuti A, Reiner O, Richards S, Victoria MF, Zhang FP, et al. Identification of a gene (FMR-1) containing a CGG repeat coincident with a breakpoint cluster region exhibiting length variation in fragile X syndrome. Cell. 1991; 65:905–914. [PubMed: 1710175]

Vestergaard M, Madsen KS, Baare WF, Skimminge A, Ejersbo LR, Ramsoy TZ, Gerlach C, Akeson P, Paulson OB, Jernigan TL. White matter microstructure in superior longitudinal fasciculus associated with spatial working memory performance in children. J Cogn Neurosci. 2011; 23:2135–2146. [PubMed: 20964591]

Wakana S, Caprihan A, Panzenboeck MM, Fallon JH, Perry M, Gollub RL, Hua K, Zhang J, Jiang H, Dubey P, Blitz A, van Zijl P, Mori S. Reproducibility of quantitative tractography methods applied to cerebral white matter. Neuroimage. 2007; 36:630–644. [PubMed: 17481925]

Wakana S, Jiang H, Nagae-Poetscher LM, van Zijl PC, Mori S. Fiber tract-based atlas of human white matter anatomy. Radiology. 2004; 230:77–87. [PubMed: 14645885]

Wang H, Ku L, Osterhout DJ, Li W, Ahmadian A, Liang Z, Feng Y. Developmentally-programmed FMRP expression in oligodendrocytes: a potential role of FMRP in regulating translation in oligodendroglia progenitors. Hum Mol Genet. 2004; 13:79–89. [PubMed: 14613971]

Wang JY, Abdi H, Bakhadirov K, Diaz-Arrastia R, Devous MD Sr. A comprehensive reliability assessment of quantitative diffusion tensor tractography. Neuroimage. 2012a; 60:1127–1138. [PubMed: 22227883]

Wang JY, Bakhadirov K, Abdi H, Devous MD Sr, Marquez de la Plata CD, Moore C, Madden CJ, Diaz-Arrastia R. Longitudinal changes of structural connectivity in traumatic axonal injury. Neurology. 2011; 77:818–826. [PubMed: 21813787]

Wang JY, Hessl DH, Hagerman RJ, Tassone F, Rivera SM. Age-dependent structural connectivity effects in fragile×premutation. Arch Neurol. 2012b; 69:482–489. [PubMed: 22491193]

Wechsler, D. Manual. San Antonio: The Psychological Corporation; 1997a. Wechsler Adult Intelligence Scale - Third Edition.

Wechsler, D. Wechsler Memory Scale Memory. 3rd ed. USA: Psychological Press; 1997b.

Zahr NM, Rohlfing T, Pfefferbaum A, Sullivan EV. Problem solving, working memory, and motor correlates of association and commissural fiber bundles in normal aging: a quantitative fiber tracking study. Neuroimage. 2009; 44:1050–1062. [PubMed: 18977450]

Zalfa F, Eleuteri B, Dickson KS, Mercaldo V, De Rubeis S, di Penta A, Tabolacci E, Chiurazzi P, Neri G, Grant SG, Bagni C. A new function for the fragile X mental retardation protein in regulation of PSD-95 mRNA stability. Nat Neurosci. 2007; 10:578–587. [PubMed: 17417632]

Zimmer HD. Visual and spatial working memory: from boxes to networks. Neurosci Biobehav Rev. 2008; 32:1373–1395. [PubMed: 18603299]

$watermark-text

$watermark-text

$watermark-text

$watermark-text
$watermark-text
$watermark-text

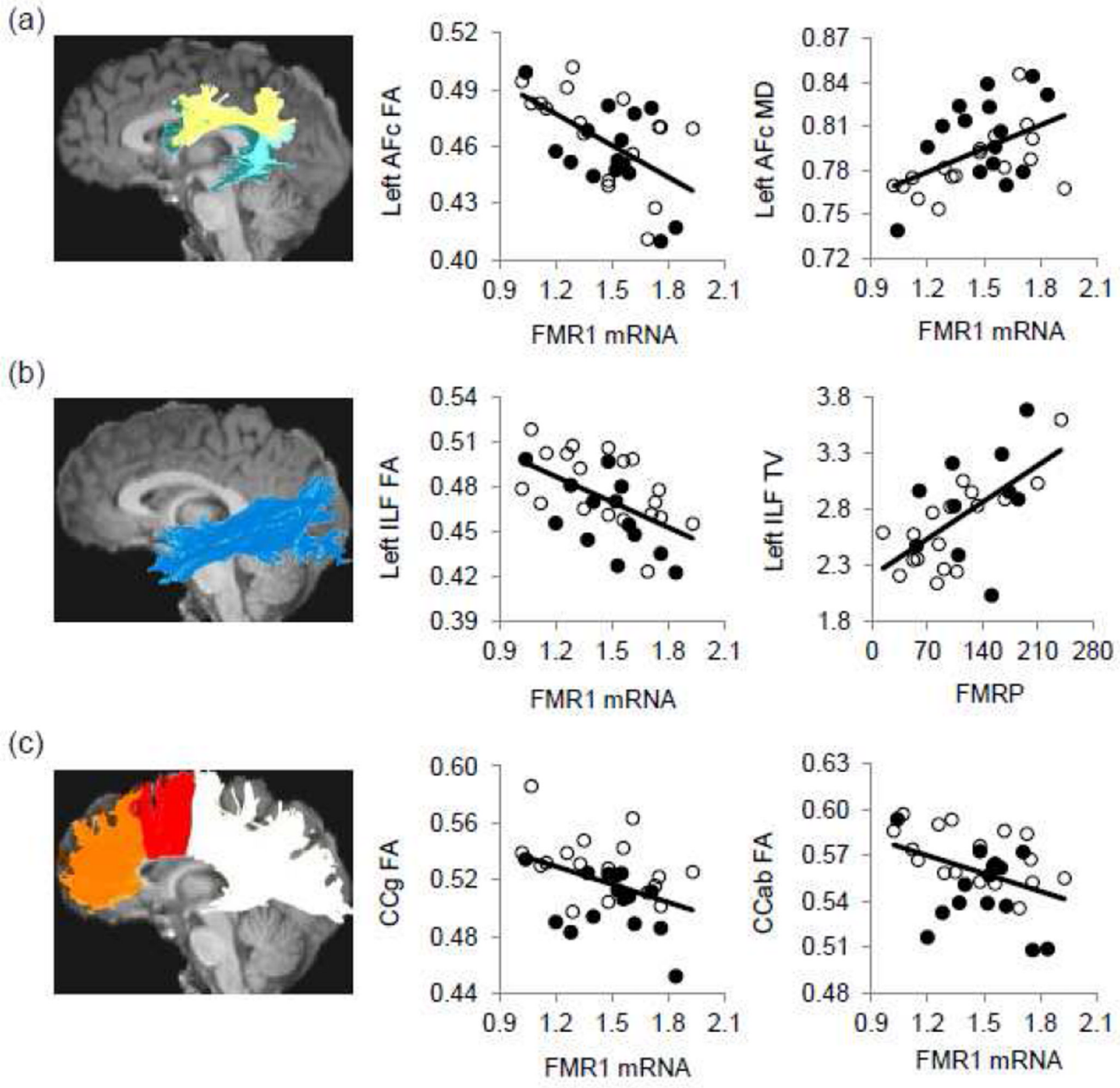

Figure 1.

The reconstructed fiber tracts and their selective associations with the *FMR1* gene expression. Fiber tracts are superimposed on a sagittal slice of the T1-weighted image. Only the left side is shown. The original data (without age adjustment) are shown. (**a**) The arcuate fasciculus complex (AFc) contains three components, namely the anterior (light yellow), posterior (aqua), and direct (dark teal) components. The FA and MD of left AFc showed significant correlation with *FMR1* mRNA. (**b**) The FA of left ILF showed significant correlation with *FMR1* mRNA. Its tract volume (TV) showed significant correlation with FMRP. (**c**) The FA of CCg (orange,) and CCab (red) showed significant correlation with *FMR1* mRNA. Measurements of MD are in μm^2/ms and tract volume in 1,000 voxels. Black dots, older participants; white dots, younger participants.

$watermark-text
$watermark-text
$watermark-text

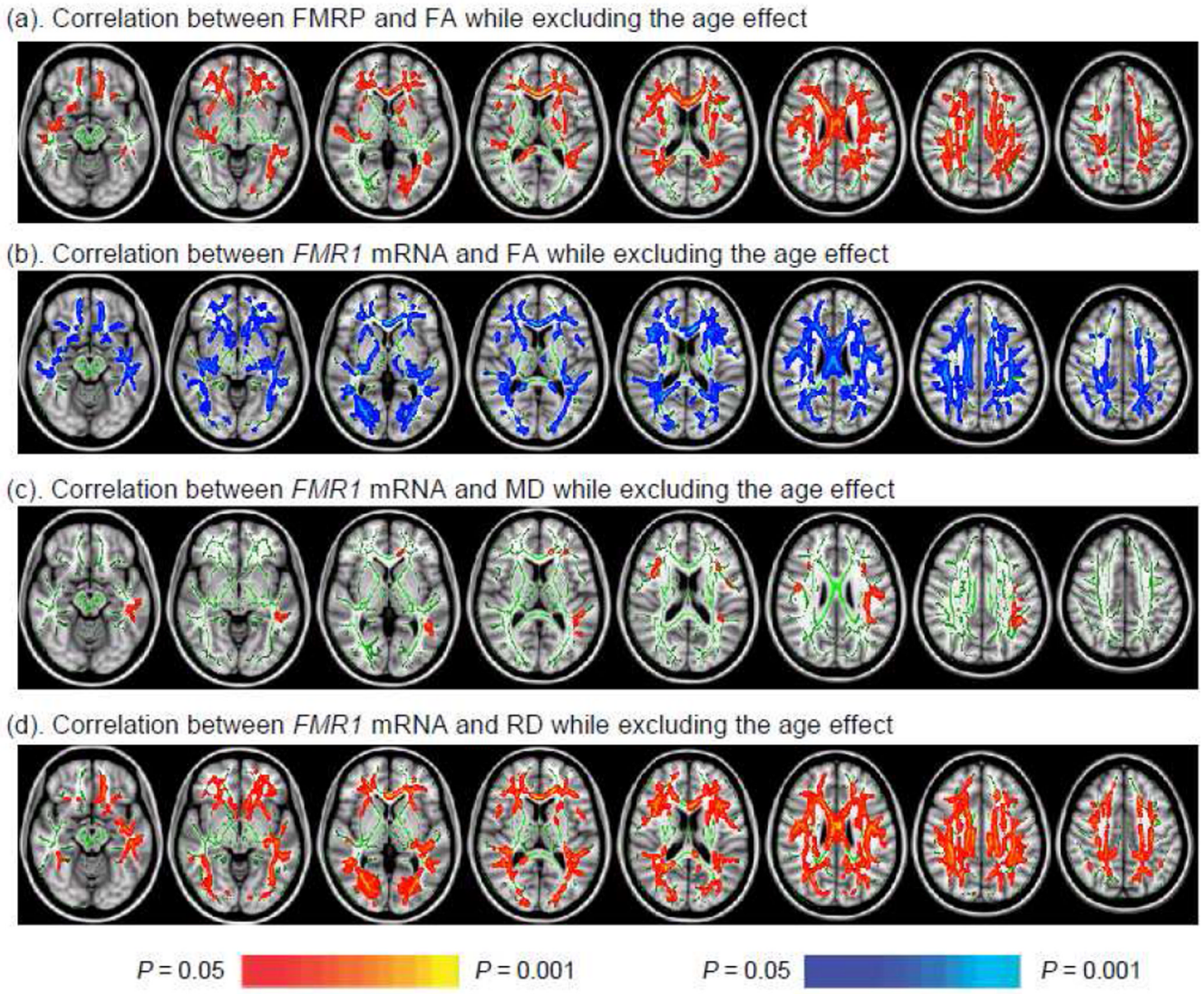

Figure 2.

TBSS showed significant associations between *FMR1* gene expression and DTI parameters. (**a**) The association between FMRP and FA was positive and widespread sparing only right internal capsule, cerebellar peduncles and fornix; (**b**) The negative association between *FMR1* mRNA and FA showed in all white matter core areas except fornix and cerebellar peduncles; (**c**) The positive association between *FMR1* mRNA and MD shown in the left ILF, bilateral arcuate fasciculus, and CCg; (**d**) The positive association between *FMR1* mRNA and RD showed in similar areas as (b).

$watermark-text
$watermark-text
$watermark-text

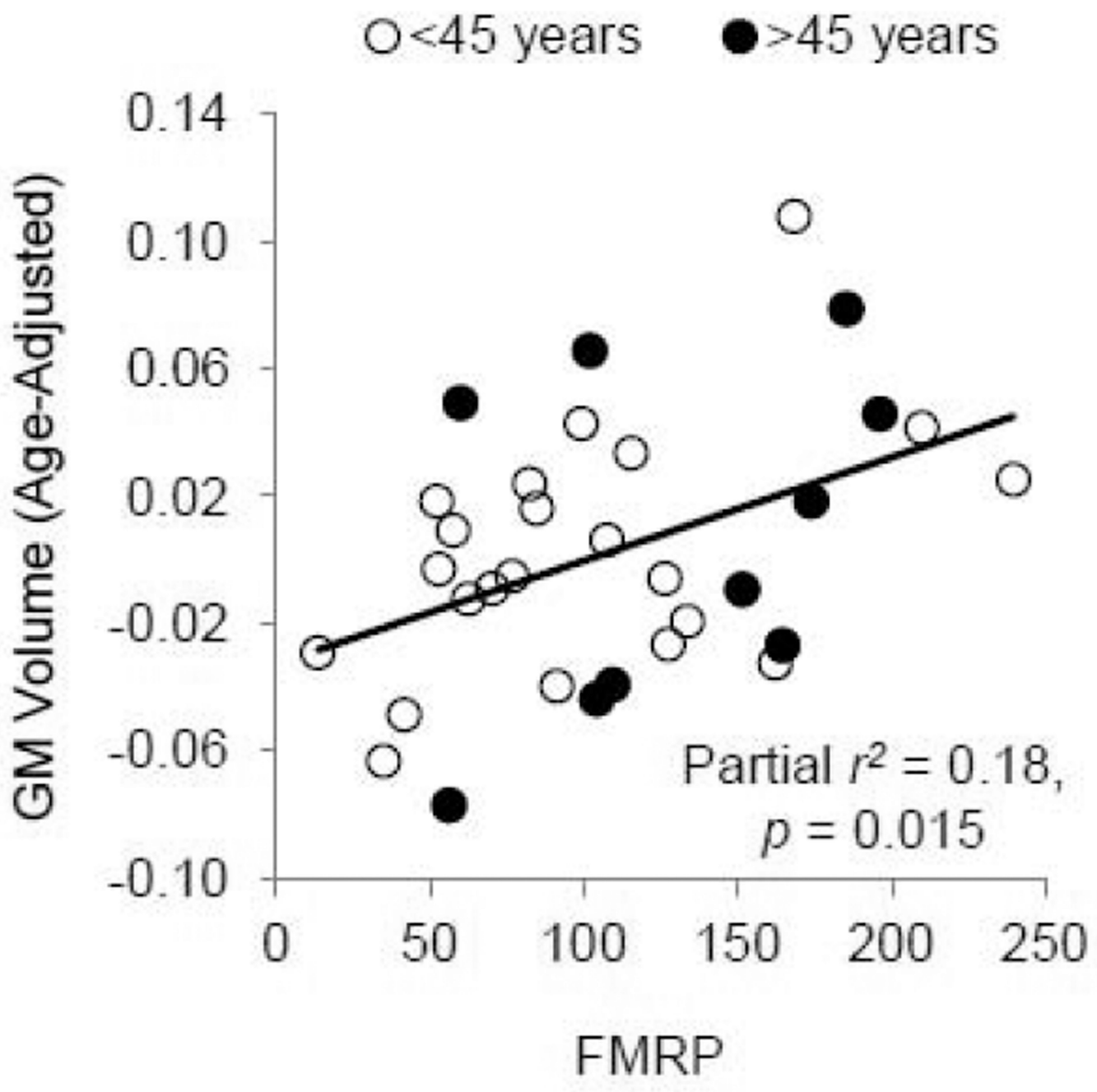

Figure 3.
The positive FMRP effect on gray matter (GM) volume. GM volume −0.06 after age-adjustment roughly corresponds to 0.56 l, 0.02 to 0.68 l, and 0.10 to 0.80 l. As there were no age-related changes in FMRP, the scatter plot produced using age-adjust FMRP look similar.

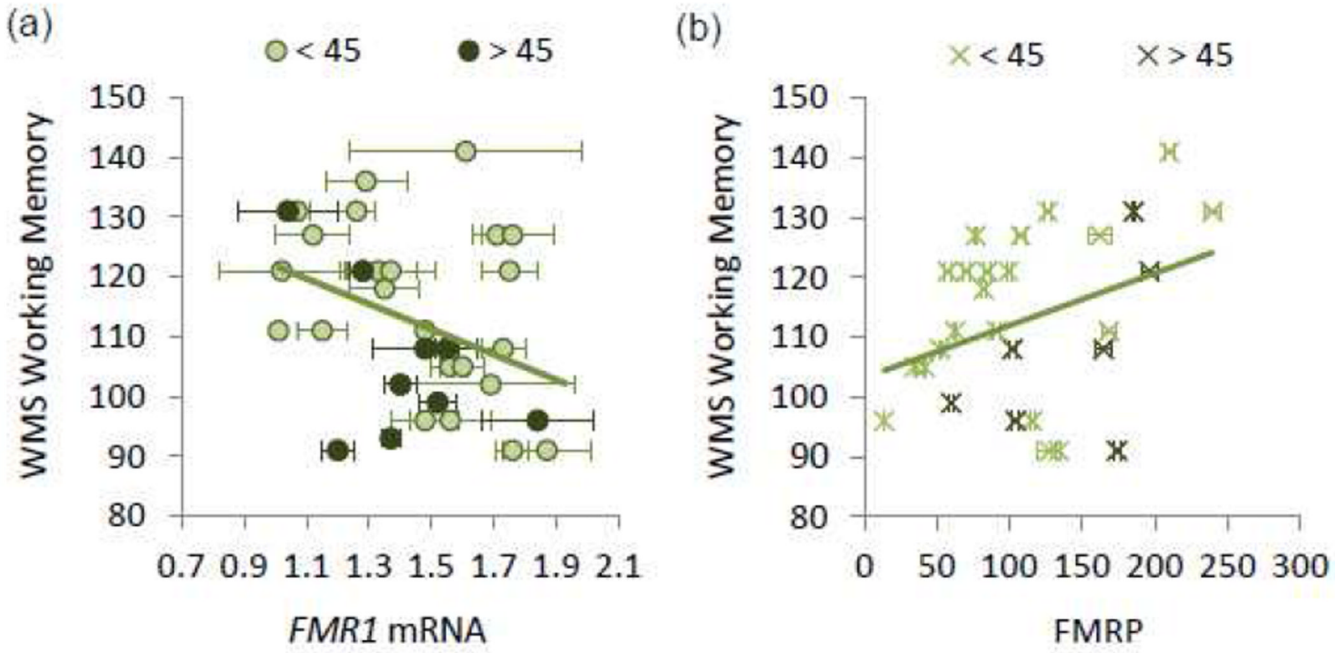

Figure 4.

Correlation of *FMR1* mRNA and FMRP with working memory performance ($n = 29$). (**a**) *FMR1* mRNA showed a negative correlation with working memory performance; (**b**) FMRP showed a positive correlation with working memory performance. Error bars indicate ±1 standard error.

$watermark-text
$watermark-text
$watermark-text

$watermark-text

$watermark-text

$watermark-text

Table 1

The participants' demographic information.

	N	Mean	SD	Range
Age	*37*	40.7	17.3	18–80
CGG Length	*37*	28.3	4.47	19–42
FMRP	*32*	109.7	56.1	13.6–239.7
FMR1 mRNA Level	*37*	1.48	0.26	1.01–1.95
WMS Working Memory	*32*	112.4	14.6	91–141

$watermark-text $watermark-text $watermark-text

Table 2

Predicting tractography measurements using *FMR1* mRNA or protein levels.

Fiber Tracts and Measurements	Descriptive (*N* = 32)		*FMR1* mRNA as a Predictor (*N* = 32)				FMRP as a Predictor (*N* = 27)			
			Age		*FMR1* mRNA		Age		FMRP	
	Mean	*SD*	Partial r^2	*P*	Partial r^2	*P*	Partial r^2	*P*	Partial r^2	*P*
Left Arcuate Fasciculus Complex										
Tract volume	2,453	640	0.08	0.12	0.01	0.56	0.07	0.20	0.00	0.46
FA	0.46	0.024	0.06	0.20	0.34	**<0.001**$^-$	0.11	0.10	0.19	0.03
MD	0.79	0.027	0.14	0.03	0.29	**0.002**$^+$	0.14	0.06	0.14	0.04
Right Arcuate Fasciculus Complex										
Tract volume	1,937	462	0.15	0.03	0.02	0.41	0.14	0.06	−0.02	0.61
FA	0.46	0.028	0.16	0.03	0.15	0.03	0.25	**0.010**$^-$	0.14	0.27
MD	0.79	0.032	0.17	0.02	0.13	0.05	0.24	**0.011**$^+$	0.20	0.02
Left Anterior Cingulum										
Tract volume	163	57	0.00	0.97	0.05	0.22	0.02	0.51	0.16	0.05
FA	0.60	0.065	0.05	0.21	0.14	0.04	0.09	0.14	0.17	0.03
MD	0.78	0.062	0.11	0.06	0.13	0.05	0.01	0.55	−0.08	0.87
Right Anterior Cingulum										
Tract volume	195	61	0.04	0.28	0.02	0.48	0.04	0.35	0.04	0.44
FA	0.55	0.059	0.26	**0.003**$^-$	0.15	0.03	0.32	**0.003**$^-$	0.17	0.04
MD	0.75	0.053	0.09	0.11	0.08	0.12	0.05	0.27	0.04	0.14
Left Inferior Longitudinal Fasciculus										
Tract volume	3,557	807	0.03	0.39	0.05	0.21	0.02	0.48	0.36	**0.001**$^+$
FA	0.47	0.026	0.17	0.02	0.35	**<0.001**$^-$	0.19	0.03	0.22	**0.013**$^+$
MD	0.83	0.030	0.27	**0.003**$^+$	0.28	**0.002**$^+$	0.18	0.03	0.08	0.04
Right Inferior Longitudinal Fasciculus										
Tract volume	3,846	987	0.02	0.49	0.02	0.46	0.01	0.58	0.29	**0.004**$^+$
FA	0.47	0.026	0.11	0.07	0.22	**0.007**$^-$	0.22	0.02	0.20	0.06
MD	0.82	0.033	0.17	0.02	0.13	0.04	0.19	0.03	0.15	0.03

$watermark-text $watermark-text $watermark-text

Fiber Tracts and Measurements	Descriptive (*N* = 32)		*FMR1* mRNA as a Predictor (*N* = 32)				FMRP as a Predictor (*N* = 27)			
			Age		*FMR1* mRNA		Age		FMRP	
	Mean	*SD*	Partial r^2	*P*	Partial r^2	*P*	Partial r^2	*P*	Partial r^2	*P*
Corpus Callosum Genu										
Tract volume	3,908	1183	0.54	**<0.001**$^-$	0.04	0.30	0.53	**<0.001**$^-$	0.01	0.35
FA	0.52	0.025	0.26	**0.003**$^-$	0.24	**0.006**$^-$	0.45	**<0.001**$^-$	0.38	**0.004**$^+$
MD	0.90	0.070	0.54	**<0.001**$^+$	0.04	0.31	0.51	**<0.001**$^+$	−0.05	0.10
Corpus Callosum Anterior Body										
Tract volume	2,563	715	0.40	**<0.001**$^-$	0.03	0.34	0.45	**<0.001**$^-$	0.16	**0.009**$^+$
FA	0.56	0.024	0.27	**0.003**$^-$	0.23	**0.006**$^-$	0.30	**0.004**$^-$	0.14	0.09
MD	0.80	0.045	0.32	**0.001**$^+$	0.02	0.46	0.21	0.02	−0.14	0.51

Bold: significant correlation at 5% FDR ($p = 0.013$) in multiple linear regression using age as a covariate;

$^+$: positive correlation;

$^-$: negative correlation.

$watermark-text $watermark-text $watermark-text

Table 3

Predicting global brain measurements using *FMR1* mRNA or FMRP.

Brain Global Measurements	Descriptive			*FMR1* mRNA as a Predictor					FMRP as a Predictor				
					Age		*FMR1* mRNA			Age		FMRP	
	N	Mean	SD	*N*	Partial r^2	*P*	Partial r^2	*P*	*N*	Partial r^2	*P*	Partial r^2	*P*
Gray matter volume (l)	*37*	0.67	0.061	*37*	0.43	**<0.001**$^-$	0.10	0.07	*32*	0.50	**<0.001**$^-$	0.18	**0.015**$^+$
White matter volume (l)	*37*	0.61	0.058	*37*	0.07	0.11	0.01	0.53	*32*	0.08	0.11	0.03	0.32
White matter FA	*32*	0.43	0.020	*32*	0.12	0.05	0.12	0.05	*27*	0.25	**0.009**$^-$	0.17	0.50
white matter MD (μm^2/ms)	*32*	0.76	0.032	*32*	0.24	**0.005**$^+$	0.05	0.22	*27*	0.12	0.08	<0.01	0.22
Gray matter MD (μm^2/ms)	*32*	1.01	0.064	*32*	0.58	**<0.001**$^+$	0.02	0.40	*27*	0.51	**<0.001**$^+$	<0.01	0.57

Bold: significant correlation at 5% FDR ($p = 0.015$) in multiple linear regression using age as a covariate;

$^+$: positive correlation;

$^-$: negative correlation.